ZnS Nanoparticle Gels for Remediation of Pb²⁺ and Hg²⁺ Polluted Water

Irina R. Pala and Stephanie L. Brock*

Department of Chemistry, Wayne State University, 5101 Cass Avenue, Detroit, Michigan 48202, United States

Ⓢ *Supporting Information*

ABSTRACT: ZnS nanoparticle (NP) gel networks were used as cation exchange materials for the removal of Pb²⁺ and Hg²⁺ from aqueous solutions. First, the suitability of the gel as a remediation material was studied by analyzing the mechanism of the cation exchange reaction. ZnS NP gels can exchange with other divalent cations (Pb²⁺, Hg²⁺) under mild reaction conditions. The speed of the reaction is influenced by the reduction potential of the incoming cation. The ZnS aerogels can remove Pb²⁺ and Hg²⁺ from aqueous solutions with a wide range of initial concentrations. For initial Pb²⁺ concentrations of 100 ppb, the Pb²⁺ concentration can be reduced below the action limit established by the EPA (15 ppb). Under thermodynamically forcing conditions, the water remediation capacity of the ZnS NP aerogels was determined to be 14.2 mmol Pb²⁺/ g ZnS aerogel, which is the highest value reported to date.

KEYWORDS: *metal contaminant, water remediation, nanomaterials, aerogel, cation exchange*
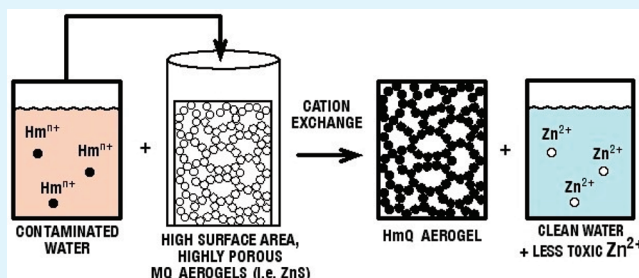
■ INTRODUCTION

The increase in the industrialization level of the world, beneficial in so many ways, also comes with a slew of drawbacks. One of the most prominent and pressing issues is the environmental deterioration that accompanies industrial processes.[1,2] For example, the heavy metal content in aquatic ecosystems increases constantly from sources such as domestic wastewater effluents (As, Cr, Cu, Mn, and Ni), coal-burning power plants (As, Hg, and Se), metallurgy (Cd, Ni, Pb, Mo, Se, and Sb) and the dumping of sewage sludge (As, Mn, and Pb).[1] Heavy metal contaminants are especially detrimental to the environment since they do not degrade over time and thus need to be physically removed from the contaminated sites. At the same time as industrial chemical use is rising, so is the demand for clean water. Accordingly, regulatory agencies in Europe and North America are imposing stricter rules for contaminated water discharge levels. Currently, the discharge levels are at parts per billion (ppb) but are expected to be reduced to parts per trillion (ppt) in the very near future, to counteract the overall increase in the pollution sources.

Current methods used for heavy-metal removal from water, such as precipitation as hydrated metal oxides or hydroxides, usually yield large amounts of contaminant-containing sediments, formed due to flocculation or coagulation.[3] Moreover, even after precipitation, the concentration levels of some heavy metals are well above those considered to be safe and acceptable today (i.e., the Environmental Protection Agency's 15 ppb action level for Pb or the maximum allowed concentration of 2 ppb Hg in drinking water). Ion-exchange provides a way to remove all ions of interest from a solution, while at the same time physically separating the contaminant.[3]

Water remediation processes using ion exchange materials are dominated by oxidic inorganic clays[4,5] or zeolites.[6] These materials have complex compositions that only allow for a limited theoretical cation exchange capacity (i.e., up to 1 mmol of exchangeable cation/g of exchanging material). Also, because of their mostly oxidic framework, they suffer from low binding affinity and selectivity for softer heavy metals. To improve the exchange capacity and affinity toward heavy metals, researchers have developed new materials by functionalizing oxidic materials (layered or porous) with softer Lewis-basic thiol groups.[7−10] The functionalization supplements the ion exchange ability with chemisorption at the surface thiol groups, resulting in improved affinity (up to 2 mmol/g exchanger) and selectivity for Hg²⁺, but not so much for other heavy metals (i.e., Pb²⁺ and Cd²⁺). Sulfide-based ion exchange materials should be ideal candidates for heavy-metal remediation applications due to their soft basic frameworks, which should show increased affinity toward softer Lewis acids (heavy metal ions such as Hg²⁺, Pb²⁺, and Cd²⁺). Surprisingly, there are just a few reports[11−19] on the soft heavy-metal-exchange properties of metal sulfides (typically layered phases), but they all show improved affinity and capacities relative to oxides.

Although porous crystalline solids and layered phases can undergo facile cation exchange, exchange in nonporous three-dimensional materials is impeded by the slow kinetics of cation diffusion through the crystal lattice.[20] Thus, cation exchange is reduced in dense bulk metal chalcogenides, even though

thermodynamically favored when systems with appropriate solubility constants are used. In nanoparticle systems, the size of the particles is similar to the reaction front size,[21] and the reaction occurs completely and at much faster rates. Thus, CdSe nanoparticles readily exchange Cd^{2+} for Ag^+.

In this report, we analyze the suitability of ZnS nanoparticle gel networks for use as Pb^{2+} and Hg^{2+} remediation materials via the easy cation-exchange chemistry previously demonstrated in our group for CdSe systems.[22] The cation exchange process occurring in the soft metal sulfide aerogels, combined with the high porosity and high surface area inherent to aerogels, should allow for increased Pb^{2+} and Hg^{2+} removal capacities when compared to the reported oxidic and even layered sulfide materials, where most of the removal occurs through chemisorption to the accessible surface. Indeed, chalcogenide aerogels based on molecular frameworks have been proven suitable for remediation.[16] However, the efficacy of their nanoparticle aerogel analogs has yet to be tested.

A schematic representation of the proposed Pb^{2+} and Hg^{2+} water remediation protocol is shown in Figure 1. Assuming that
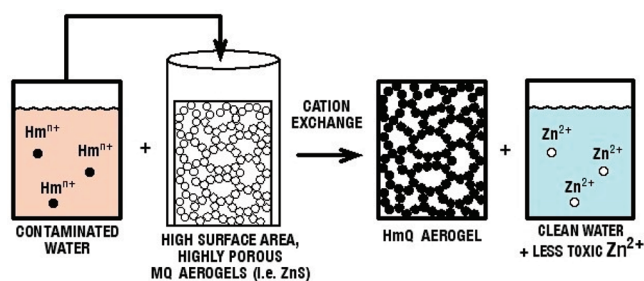
Figure 1. Schematic representation of the Pb^{2+} or Hg^{2+} (Hm) water remediation process using metal chalcogenide (MQ) aerogels.

the cation exchange process will occur in a mole−to−mole ratio, a theoretical capacity of 2127 mg Pb/g ZnS aerogel (10.3 mmol/g) is predicted. This is almost an order of magnitude higher than the highest capacities reported to date, 331 mg/g (1.6 mmol/g) for a zinc sulfide chalcogel[16] or 365 mg/g (1.8 mmol/g) for thiol functionalized oxidic materials.[7]

In this paper we report the following: (1) ZnS nanoparticle aerogels can remove Pb^{2+} and Hg^{2+} from aqueous solutions in a direct, one-step cation-exchange reaction, under very mild reaction conditions; (2) the capacity of ZnS aerogel for Pb^{2+} removal can be as high as 2950 mg Pb/g exchanger (14.2 mmol/g); (3) the concentration of Pb^{2+} in an aqueous waste simulant can be reduced below the EPA recommended 15 ppb action level.

■ EXPERIMENTAL SECTION

Synthesis of ZnS Wet Gels. Colloidal ZnS nanoparticles (NPs) were synthesized using the inverse micellar route.[23−25] In a typical synthesis, 111.53 g (0.25 mols) of sodium bis(ethylhexyl) sulfosuccinate (AOT) was dissolved in 477.5 mL n-heptane. This solution was divided into two round-bottom flasks and 11.25 mL of 0.15 M aqueous solutions of $Zn(NO_3)_2$ and Na_2S were added to each flask, creating the inverse micelle nanoreactors in which the reaction would occur. The solutions were then degassed under vacuum and purged with Ar gas. After 1 h of stirring to achieve homogeneity, the sulfide solution was cannulated into the zinc solution and the resultant zinc sulfide was stirred overnight. The surfactant groups were then exchanged by adding 1.8 mL of 4-fluorothiophenol (FPhSH) and 2 mL of triethylamine (TEA), causing the nanoparticles (NPs) to precipitate from solution. The NPs were isolated by centrifugation,

washed with hexanes, and dispersed in 20 mL of acetone. The colloidal NPs were then assembled into 3D wet gel networks by adding 0.2 mL aliquots of 3% tetranitromethane (TNM) solution in acetone to each 4 mL aliquot of ZnS NP sol. The wet gels were left to age for 1 week, and the solvent was then exchanged with fresh acetone 2−3 times a day over a 2 day period.

Drying of the Gel Networks. The wet gels were transformed into aerogels or xerogels using supercritical carbon dioxide drying (SCD) or benchtop drying, respectively. To produce aerogels, the wet gel monoliths were dried in glass vials, with a punctured polyethylene cap to allow for solvent exchange within the SPI-DRY model critical point dryer. The acetone was exchanged with liquid CO_2 over a 4 h period. The CO_2 was then rendered supercritical by raising the temperature to 39 °C, with a concomitant pressure increase to ~1500 psi. The samples were kept at this temperature for 1 h and the CO_2 gas was then bled out of the chamber at a rate of 50−100 psi/min, to minimize pore collapse and yield the highly porous aerogel material. Alternatively, the gels were dried under ambient conditions by evaporating the liquid from the pores in open vials on the benchtop. In this instance, the pore structure of the wet gel collapses under the influence of the evaporating solvent's capillary forces on the pore walls, yielding a xerogel.

Cation Exchange of ZnS Gel Networks. The initial cation exchange study was conducted by adding 4 mL of 150 mM $Cd(NO_3)_2$ in methanol or $Pb(NO_3)_2$ in 1:1 V/V methanol: water solutions (representing an approximate 3 fold excess) to ZnS wet gels that were previously exchanged with fresh methanol. The cation exchange process was conducted for various amounts of time (overnight for Pb^{2+} and over 2 weeks for Cd^{2+}), followed by exchange with fresh solvent, supercritical drying, and analysis of the resultant gels. In a parallel study, similar volumes of the exchange cation aqueous solutions were added to dry aerogels and xerogels, to test their exchangeability for water remediation applications.

Powder X-ray Diffraction (PXRD) Measurements. A Rigaku RU 200B powder diffraction instrument using Cu K_α (λ = 1.514 Å) radiation (rotating anode source operating at 40 mV and 150 mA) was used to obtain diffraction intensity data. The dry aerogel, xerogel or NP samples were placed on a zero background quartz holder with the use of a small amount of silicone grease. The diffraction peaks were indexed relative to phases in the International Center for Diffraction Data (ICDD) Powder Diffraction File (PDF) database (release 2000).

Transmission Electron Microscopy (TEM) Imaging and Energy-Dispersive X-ray Spectroscopy (EDS). The aerogel microstructure was imaged using TEM and the relative atomic composition was determined using EDS. The samples were sonicated in acetone and placed on a carbon-coated copper grid (SPI). A JEOL FasTEM 2010 HR microscope with acceleration voltage of 200 kV was used. High-resolution TEM (HRTEM) micrographs were collected for representative samples. The TEM is equipped with an EDAX EDS detector for elemental analysis.

Quantitative Pb^{2+} and Hg^{2+} Uptake Studies. The Pb^{2+} and Hg^{2+} uptake from solutions of various concentrations was determined using the batch method at $V/m \approx 1000$ mL solution/1 g solid exchanger, where V is the solution volume in mL and m is the mass of the ZnS solid exchanger used, in grams. In a typical experiment, 10 mL aqueous (HPLC grade water) solutions of the metal of interest (i.e., Pb^{2+}, Hg^{2+}) of various initial concentrations was added to 10 mg of ZnS aerogel or xerogel. The mixture was kept undisturbed or stirred at room temperature for a specific time. The mixture was then centrifuged and an aliquot of solution taken out carefully, to avoid removing solid particles. The aliquots were then diluted with 2% nitric acid in HPLC grade water and the metal content was analyzed with ICP-MS. Competitive ion exchange experiments were also performed with the batch method with a V/m ratio of 1000 mL/g at room temperature and a contact time of 24 h. The competing ions (i.e., Na^+, Ca^{2+}, and Mg^{2+}) were added in a 1000 fold excess to the metal tested (1 M competing ion vs 1 mM Pb^{2+} or Hg^{2+}) and the experiments were carried out the same as described above. The material was also tested with tap water that was spiked with the metal ion of interest to mimic more real-life conditions. For each sample, a control test without

adsorbent was also conducted, to normalize for possible metal precipitation.

The affinity and selectivity of the ZnS material for the metal ion tested is expressed using the distribution coefficient K_d, calculated with the equation $K_d = (V/m)[(C_0 - C_f)/C_f]$, where C_0 and C_f are the initial and final metal ion concentrations in units of ppm (mg/L) or ppb (μg/L), V is the testing solution volume (mL) and m is the amount of solid exchanger (g) used in the experiment. Also, the capacity, q_e, of the aerogel for Pb^{2+} or Hg^{2+} removal was calculated using the equation $q_e = (V/m)(C_0 - C_f)$, with the variables defined the same as above, but with C_0 and C_f expressed in ppm, and V expressed in L.

Inductively Coupled Plasma Mass Spectrometry (ICP-MS) Measurements. Metal concentrations were measured with a Perkin-Elmer Life Sciences Elan 9000 instrument equipped with an automatic sampler. The data were collected as counts per second. A standard external calibration curve was constructed from diluted stock solutions of 1000 ppm standards (High-Purity Standards) with 2% (by volume) concentrated HNO_3 in HPLC grade water. Four calibration standards from 1 to 20×10^{-3} ppm were prepared. The calibration curves were linear with less than 0.1% deviation. The samples were also diluted before measurements with 2% (by volume) concentrated HNO_3 to yield metal concentrations within the calibration range and the concentrations of the targeted metals were measured before and after treatment with the ZnS aerogel. Isotopes ^{208}Pb, ^{202}Hg, ^{64}Zn, and ^{66}Zn were analyzed. For each sample, three readings of the ICP-MS intensity were recorded and averaged. Standards were measured before and after the samples to analyze for instrument drift. Blank samples were analyzed periodically between samples, to check for sampling probe contamination.

Error Determination. The weight of the ZnS aerogel used for Pb^{2+} or Hg^{2+} remediation was determined with an analytical balance with ±0.1 mg precision. In a typical experiment, the amount of ZnS aerogel used was between 5 and 11 mg. This introduced an error of approximately 2% in the final calculation of capacity and distribution coefficient.

The samples collected after the Pb^{2+} or Hg^{2+} remediation experiments were iteratively diluted to the low ppb levels required by the ICP-MS analytical technique used. The dilution skill of the human operator was determined by preparing duplicate samples of each collected sample. The samples were then separately analyzed, and the results reported as an average value and standard deviation.

The instrument error or drift over time was also determined by analyzing the same samples twice over a few hours' interval. The experiment was repeated at least twice for each initial concentration and the results were then reported as the average value of the measurements and standard deviation.

RESULTS AND DISCUSSION

Sol–gel chemistry enables the creation of solid networks in which semiconducting metal chalcogenide NPs (e.g., CdSe, CdTe, PbS, or ZnS) are linked together into a highly porous 3D network (wet gel), without organic ligands at the interfaces between particles.[26,27] Supercritical drying leads to an aerogel material wherein high porosity and dual particle/void interconnected networks enable the fast and efficient movement of matter through the structure and to the NP surfaces.[28]

We have recently demonstrated[29] that the chalcogenide gel network is held together by covalent di- or poly-selenide bonds, enabling cation exchange to occur without destroying the 3D gel network. The validity of this hypothesis has been tested[22] through the conversion of CdSe gels into Ag_2Se, PbSe, and CuSe simply by immersing an already gelled CdSe wet gel monolith in the cation solution of choice. The exchange resulted in complete conversion, whereas the monoliths remained intact.

The current study presents the extension of the cation-exchange chemistry to ZnS gel networks for the purpose of evaluating their suitability for removal of Cd^{2+}, Pb^{2+} or Hg^{2+}

from contaminated aqueous solutions. The cation exchange is thermodynamically favored by differences in solubility between the incoming and outgoing cations and, at the nanoscale, the activation barrier of the process is also lowered, creating fast kinetics that allow the rapid diffusion of ions in the lattice framework.[21] We chose to investigate ZnS, as opposed to the already reported CdSe, because Zn^{2+} and S^{2-} are less toxic than Cd^{2+} and Se^{2-}, respectively.[30]

As a first step, we probed whether the direct exchange between divalent cations previously studied in CdSe aerogel materials[22] can be extended to ZnS aerogels, as well as the speed of the exchange, because practical applications in water remediation would require reasonably fast kinetics. To interrogate which factors are the main reaction driving forces in our system, we compared Pb^{2+} and Cd^{2+} as the incoming exchanging cations, since their sulfides have similar solubility product constants (K_{sp}): $K_{sp} = 3.2 \times 10^{-33}$ for PbS, and 5.0×10^{-34} for CdS. These values are similar, and lower than that for ZnS ($K_{sp} = 1.3 \times 10^{-29}$), rendering the exchange reaction thermodynamically favored by similar energy differences.[31]

Wet gels of ZnS were treated with solutions of Pb^{2+} and Cd^{2+} under forcing conditions (3 fold excess of exchanging ion) and the process monitored visually by the gel color change. Results indicate (Figure 2) that the Zn^{2+} cation can be exchanged with

Figure 2. Pictures of a (left) ZnS wet gel and (middle) Cd^{2+}- and (right) Pb^{2+}-exchanged wet gels, showing the specific color change and the conservation of the 3D gel monolith integrity upon the cation exchange. (The size of the monoliths is not to scale, nor does it represent a series in which a particular ZnS monolith was exchanged).

Pb^{2+} and Cd^{2+} upon treatment of ZnS wet gels with solutions containing these ions, in a one-step cation exchange reaction, under very mild conditions (room temperature, methanol (Cd) or methanol/water (Pb) solvent).

A first observation was that the time scale of the exchange was very different for the two ions: the exchange between Pb^{2+} and Zn^{2+} (color change from white ZnS to black PbS) happened in less than one minute while the characteristic yellow color of CdS did not appear until several days later. For both systems, the gel networks remained undisturbed (Figure 2), as previously observed in the selenide systems.[22] PXRD data for the xerogels resulting from exchange with Pb^{2+} overnight and with Cd^{2+} for two weeks show that the incoming metal cation has been incorporated into the lattice, generating PbS and CdS (Figure 3) and that crystallinity was preserved as the structure changes. The peak sharpness increases for the faster Pb^{2+} exchange, indicating that the crystallite size had increased. Using the Scherrer equation,[32] the crystallite size can be calculated to be 4.3 nm for ZnS precursor gel, 4.1 nm for the Cd^{2+}, and 18.6 nm for the Pb^{2+} exchanged gels. The small size difference observed between the ZnS and Cd^{2+}-exchanged material is indicative of the fact that during the slow exchange process, the anionic network was not, or very little, visibly disturbed. However, the fast Pb^{2+} exchange proceeds with a greater lattice rearrangement and causes the particle building blocks to grow in size. Nevertheless, the NPs maintained their
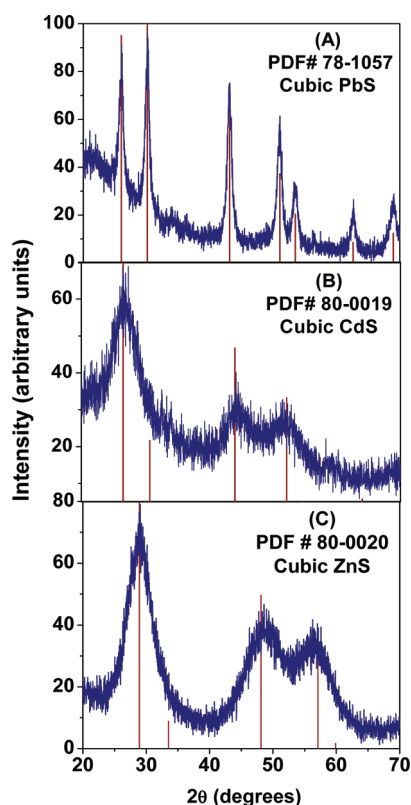
Figure 3. PXRD spectra of (A) PbS and (B) CdS xerogels resulting from exchange of ZnS wet gels with Pb^{2+} and Cd^{2+}, respectively; and (C) ZnS xerogel resultant from benchtop drying a wet ZnS gel. The vertical lines represent the respective crystal patterns, according to the PDF patterns noted in the figure.

connectivity and the integrity of the gel network was conserved (Figure 4).
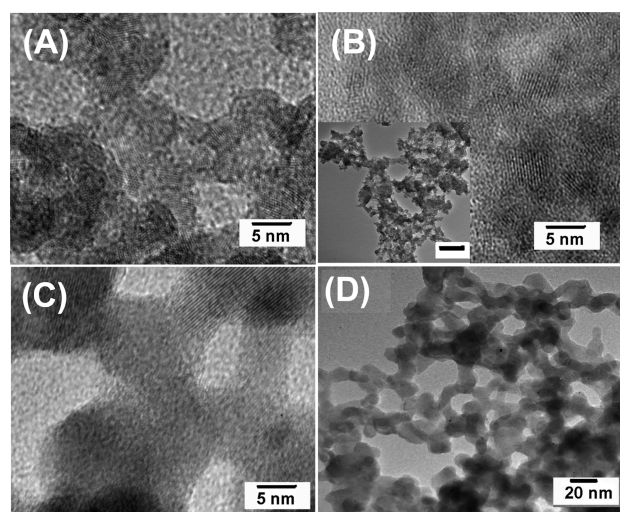
Figure 4. TEM micrographs of (A) ZnS aerogel and (B) Cd^{2+}- and (C, D) Pb^{2+}-exchanged ZnS wet gels supercritically dried to form aerogel networks. The inset in B shows a lower magnification of the Cd^{2+}-exchanged gel, with the gel network intact (scale bar 100 nm). The NP size increases during the cation exchange (B, C), but the gel network remains connected (B inset, D).

TEM images (Figure 4) confirm the retention of the gel network connectivity during exchange. The minimal increase in

NP size indicated by the PXRD data is consistent with crystallite sizes observed in TEM for starting ZnS ($\sim$4 nm) and final CdS ($\sim$5 nm) materials. Likewise, TEM reveals PbS primary particle sizes on the order of 7−15 nm, confirming the increase in crystallite size relative to ZnS noted by PXRD. EDS analyses show that not all ions exchanged equally; e.g., removal of Zn^{2+} by displacement with Cd^{2+} proved difficult to drive to completion. The reason for the incomplete cation exchange between Cd^{2+} and Zn^{2+} might stem from the known capacity of II−VI compounds for forming pseudobinary alloy systems.[33,34] On the other hand, IV−VI compounds are sparsely soluble in II−VI crystals, and thus the ion exchange of ZnS with Pb^{2+} is expected to form heterostructures, not solid solutions, leading to complete conversion, which is what we observed.

On the basis of these data, we surmise that the ion-exchange reaction occurring in the ZnS gel materials is driven by a different set of thermodynamic factors, because ions with similar solubility product constants exchange at very different rates (minutes for Pb^{2+}, days for Cd^{2+}). The speed of the exchange correlates with the difference in the reduction potential between Zn^{2+} and the incoming metal cation; i.e., the bigger the difference, the faster the exchange (Table 1).

Table 1. Solubility Product Constants, Reduction Potentials, and Observed Cation Exchange Speed for ZnS and Resultant Cation-Exchanged Aerogels

material	solubility product constant, (K_{sp})	reduction potential (E^0) of the cation (M^{n+}/M), (V)	ΔE^0 ($M^{2+}/M - Zn^{2+}/Zn$), (V)	qualitative speed of exchange
ZnS	1.3×10^{-29}	−0.763		
CdS	5.0×10^{-34}	−0.403	+0.360	weeks
PbS	3.2×10^{-33}	−0.125	+0.638	minutes
HgS	7.9×10^{-57}	+0.854	+1.617	seconds

A similar trend was previously reported[35] for the cation exchange of ZnS thin films. This trend has been justified by the fact that the low solubility and highly covalent character of metal sulfides causes the electrochemical electron transfer to have a higher importance over solubility-difference-driven conversion.

This study allowed for a better understanding of one of the factors affecting the exchange mechanism that will facilitate the optimization of the reaction conditions and the extension to other metals for remediation studies. The process should be generic and should work for any metal with a more positive standard reduction potential than that of Zn^{2+}/Zn. The trend was tested by using Hg^{2+} for the exchange ($K_{sp}= 7.9 \times 10^{-57}$, $E^0_{Hg^{2+}/Hg} = +0.854$ V). When a ZnS wet gel was treated with a solution of Hg^{2+}, the white gel turned black almost immediately, suggesting exchange for Hg^{2+} has occurred and happens more rapidly than for Pb^{2+}, as expected on the basis of the large, positive reduction potential.

The observation of the direct exchange between divalent metal cations is different from previous work on cation exchange in NP systems,[34,36−39] in which CdSe/CdS NPs were reported to be unable to directly convert to PbSe/PbS under mild reaction conditions, requiring an intermediate step of converting to Cu_2Se/Cu_2S. These previous reports justified their observations based on the assumption that the cation exchange reactions are driven mainly by the difference in solubility of the incoming and outgoing cation in various solvents and thus a direct exchange between divalent cations of similar solubility

would not be possible, requiring the intermediate singly charged ion-exchange step.

The observed ability of our material to undergo direct cation exchange between two cations with the same charge stems from the fact that, unlike the previously reported NP systems, the capping groups that are normally used to stabilize NPs are almost entirely removed in our systems during the gelation process, leaving behind a surface that is much more easily accessible to the incoming cation. Previous reports[40] have shown that the S content — indicative of the coverage of thiol surfactants used to stabilize the NPs — decreases from almost 20% for CdSe NPs to about 10% in the corresponding aerogels. Once the surface cations are exchanged, the concentration gradient created generates a reaction potential (Donnan potential[41]) that is propagated through the gel network, allowing for the complete exchange. Indeed, we find that treating a thiolate-capped ZnS NP sol with 150 mM Pb(NO$_3$)$_2$ solution (the same conditions as the wet gel exchange) required nearly a month for conversion (see Figures S1 and S2 in Supporting Information). Other studies have also shown that there is a kinetic effect that depends on the surfactant nature and concentration, where a decrease in the speed of reaction with increased surfactant concentration (i.e., surface ligation) was observed.[42,43]
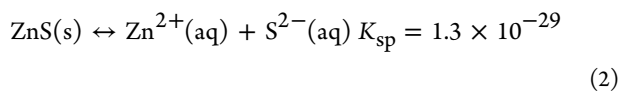
Quantitative Estimation of Pb^{2+} Removal from Aqueous Solutions by ZnS Aerogels. The qualitative study described above indicated that the ZnS gels should be suitable for the removal of both Pb^{2+} and Hg^{2+} ions from contaminated solutions. Therefore, we conducted a quantitative study of the removal efficiency of ZnS, focusing largely on aqueous Pb^{2+} solutions. Briefly, we treated ZnS aerogels with solutions containing different concentrations of Pb^{2+} ranging from 20 000 to 0.01 ppm, and measured the metal concentrations before and after treatment with ICP-MS. We kept the ratio of Pb^{2+}-contaminated solution to ZnS aerogel constant at 1000 mL of solution/1 g of aerogel for all experiments.

The measure of the ZnS aerogel's affinity for Pb^{2+} was gauged by calculating the distribution coefficient, K_d. K_d measures the exchanging material's capacity to partition the metal ion of interest between the solution and the aerogel; values larger than 500 mL/g are considered acceptable, those above 5000 mL/g are very good, and those above 50 000 mL/g are considered outstanding.[44]
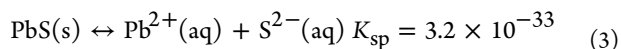
We observe three distinct behaviors corresponding to low, medium, and high Pb^{2+} concentrations as a result of the exchange thermodynamics. If we consider the overall cation exchange reaction

$$ZnS(s) + Pb^{2+}(aq) \leftrightarrow PbS(s) + Zn^{2+}(aq) \qquad (1)$$
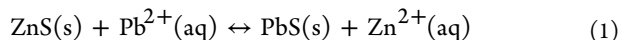
it can be thought of thermodynamically as the combination of the solubilization processes

$$ZnS(s) \leftrightarrow Zn^{2+}(aq) + S^{2-}(aq) \quad K_{sp} = 1.3 \times 10^{-29} \qquad (2)$$

and

$$PbS(s) \leftrightarrow Pb^{2+}(aq) + S^{2-}(aq) \quad K_{sp} = 3.2 \times 10^{-33} \qquad (3)$$

Thermodynamically, (1) = (2) − (3), and the equilibrium constant (K) for the cation exchange process can be derived from the solubility product constants for ZnS and PbS: $K = K_{sp\ ZnS}/K_{sp\ PbS} = 4.1 \times 10^3$. At low, nonforcing Pb^{2+}

concentrations (0.01 to 0.1 ppm), the equilibrium is limited by the native solubility of ZnS. At medium concentrations (20−200 ppm), ZnS solubility is no longer limiting and the equilibrium is more favorable for PbS formation. Finally, at high concentrations (2000−20 000 ppm), the equilibrium is forced strongly to the right, and the native solubility of PbS becomes limiting.

1. Initial Concentrations Ranging from 10 to 100 ppb. The ZnS aerogel is very effective at removing Pb^{2+} ions from solutions with low initial concentrations (up to 100 ppb Pb^{2+}), decreasing the concentration below the EPA recommended action level of 15 ppb Pb^{2+} (Table 2, Figure 5). This initial

Table 2. Initial (10−100 ppb) and Final Pb^{2+} Concentrations, Percent Removal, and Distribution Coefficient K_d (error represents instrument accuracy)

initial Pb^{2+} concentration (ppb)	final Pb^{2+} concentration (ppb)	amount of Pb^{2+} removed (mmol)	removal (%)	K_d (mL/g)
97.08 ± 0.03[a]	12.24 ± 0.06	0.0041	87.3	7.27 × 10^3
93.47 ± 0.25	9.08 ± 0.18	0.0041	90.1	9.13 × 10^3
10.15 ± 0.15	1.49 ± 0.07	0.00042	84.9	6.49 × 10^3

[a]Sample was not stirred.
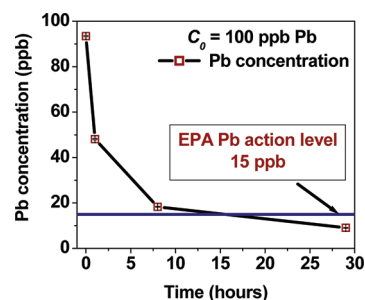
Figure 5. Decrease in Pb^{2+} concentration with time for an initial concentration of 100 ppb.

concentration range is a good mimic for an actual environmental spill, where large volumes of dilute solutions must be treated. The K_d values obtained are in the "very good" range, since the low initial concentrations are not creating thermodynamically driving conditions. However, the low final concentrations attained of Pb^{2+} in solution are encouraging for the use of ZnS aerogels in remediation.

2. Initial Concentrations Ranging from 20 to 200 ppm. In the initial concentration range from 20 to 200 ppm, the forward reaction equilibrium is favored and the ZnS aerogel proved to be the most efficient in removing Pb^{2+} ions from aqueous solutions (Table 3, Figure 6), showing "very good" to "excellent" K_d values ranging from 17 200 to 72 300 mL/g for Pb^{2+}. Nearly all of the Pb^{2+} can be removed (≥95%), but the more forcing conditions result in higher final Pb^{2+} concentrations (>50 ppb).

For similar initial Pb^{2+} concentrations, stirring the solution during the exchange contributed to a mere 3−4% increase in the percent removal (see first entry in Tables 2 and 3). This is an indication that, for all practical purposes, stirring the samples is not required.

3. Initial Concentrations Ranging from 2000 to 20 000 ppm. With initial Pb^{2+} concentrations higher (i.e., 1.5 fold Pb^{2+} excess) than the saturation value for the amount of ZnS aerogel used (if mole to mole exchange occurs) the

2164

dx.doi.org/10.1021/am3001538 | ACS Appl. Mater. Interfaces 2012, 4, 2160−2167

Table 3. Initial (20−200 ppm) and Final Concentrations, Percent Removal, and Distribution Coefficient K_d (error represents dilution accuracy)

initial Pb^{2+} concentration (ppm)	final Pb^{2+} concentration (ppm)	amount of Pb^{2+} removed (μmol)	amount of Zn^{2+} liberated (μmol)	removal (%)	K_d (mL/g)
171 ± 15^a	9.86 ± 0.3	6.45	9.14	94.5	1.72×10^4
171 ± 15	3.61 ± 0.1	7.27	11.5	98.1	5.05×10^4
13.80 ± 1.09	0.189 ± 0.01	0.545	1.65	98.6	7.23×10^4
1.26 ± 0.10	0.066 ± 0.007	0.0450	2.35	95.5	2.14×10^4

^{a}Sample was not stirred.
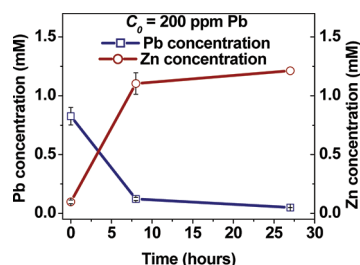
Figure 6. Decrease in Pb^{2+} and increase in Zn^{2+} concentrations as a function of contact time (error bars represent dilution accuracy). The concentrations have been converted to molarity to aid in gauging the cation exchange magnitude.

aerogel exhibits a removal capacity of 1730 ± 90 mg Pb/g ZnS exchanger, which is much higher than the previously reported capacities of 331 mg/g for a zinc tin sulfide chalcogel[16] or 365 mg/g for thiol functionalized oxidic materials,[7] and close to the theoretical capacity of 2127 mg Pb/g ZnS. If the equilibrium is pushed to the right by the use of higher excess Pb^{2+} (i.e., 5- or 10-fold), see Table 4, even higher capacities can be reached. The fact that we measured capacities that are higher than that theoretically calculated based solely on exchange suggests that Pb^{2+} is also being chemisorbed to the aerogel surface, perhaps by residual thiol groups that are still present. Under these strongly forcing conditions, the concentration of Pb^{2+} is largely governed by the PbS solubility constant and it is no longer useful to compare K_d values.

Ion-Exchange Mechanism. To discern whether the ion remediation was occurring by exchange, we also monitored the Zn^{2+} concentration for moderate to high concentrations of exchanging ion (Zn^{2+} concentrations were not measured for 0.01 to 0.1 ppm exchange experiments). The Pb^{2+} concentration decreased while the Zn^{2+} concentration increased, supporting the fact that the removal was occurring via an ion-exchange mechanism, and not merely by physisorption or chemisorption to surface thiol groups. Typical curves obtained are shown in Figure 6. We have observed that when the initial concentration of the exchanging ion was low (below full capacity of the ZnS aerogel), the moles of released Zn^{2+} were higher than those of Pb^{2+} removed (Table 3). We already know that the cation exchange takes place since we observed the formation of the PbS phase by PXRD, so we attribute this slight Zn^{2+} excess to

the dissolution of the ZnS aerogel. At the same time, there is also the possibility of a slight ZnS NP contamination due to the breakdown of the gel network. When the initial concentration was at or above full exchange capacity, the Zn^{2+} was completely replaced and the number of moles was always lower than the incoming Pb^{2+} (see Table 4). Nevertheless, the amount of Zn^{2+} ions liberated during the process was almost constant and within the range expected for the complete exchange with Pb^{2+} (0.056 mmol ZnS were used for the experiment), which indicates that the ion exchange occurred preferentially over chemisorption of Pb^{2+}. A similar observation of Pb^{2+} being absorbed above the cation exchange capacity of the material was noticed with the mineral montmorillonite[5] and was explained by the formation of small Pb nanoparticles at the surface and edges of the crystallites. However, we found no evidence of Pb formation, either in TEM, or by PXRD (see Figures 3 and 4).

Effect of Competing Ions/Porosity on Removal Efficacy. When competing ions such as Na^+, Ca^{2+}, or Mg^{2+} — which can be expected to be present in real world samples — are present in large excess (i.e., 1 M competing ion vs ~1 mM Pb^{2+}), the K_d decreases by 1 order of magnitude (Table 5). This pheno-

Table 5. Distribution Coefficients for Pb^{2+} in the Presence of Competing Ions

initial Pb^{2+} concentration (mM)	competing ion and concentration (M)	K_d for Pb^{2+} (mL/g)	previous report^a K_d (mL/g)
0.830	none	2.35×10^4	1.1–8.9×10^5
0.830	Na^+ (1 M)	1.11×10^4	8.34×10^4
0.849	Ca^{2+} (1 M)	5.58×10^3	1.88×10^4
0.835	Mg^{2+} (1 M)	2.91×10^3	n/a

^{a}The previously reported[14] K_d values were obtained by treating a layered potassium manganese sulfide with a slightly more forcing initial Pb^{2+} concentration (~1.45 mM) and a slightly lower V/m ratio (~900 mL/g) than the ones used here.

menon has been previously observed in a layered potassium manganese tin sulfide material.[14] The reason for the decrease could be the creation of electrostatic repulsion forces between the ZnS aerogel surface and the incoming cation, due to the increase in the solution's activity at these high concentrations. Nevertheless, the ZnS aerogel still showed Pb^{2+} removal of 74% in the presence of Mg^{2+}, 85% in the presence of Ca^{2+}, and 92%

Table 4. Removal Capacity and Amounts of Pb^{2+} Removed and Zn^{2+} Liberated When Using 0.056 mmol ZnS Aerogel with Solutions with Different Initial Pb^{2+} Concentrations (2000−20 000 ppm)

initial Pb^{2+} concentration (ppm)	amount of Pb^{2+} removed (mmol)	amount of Zn^{2+} liberated (mmol)	removal capacity (mg Pb/g ZnS)	removal capacity (mmol Pb/g ZnS)
24600 ± 320	0.078 ± 0.007	0.041 ± 0.009	2950 ± 270	14.2 ± 1.3
12000 ± 150	0.071 ± 0.003	0.050 ± 0.010	2680 ± 120	12.9 ± 0.58
2320 ± 27	0.046 ± 0.002	0.031 ± 0.022	1730 ± 90	8.35 ± 0.43

in the presence of Na$^+$, indicative of the strong material preference for heavier, softer cations.

ZnS xerogels (benchtop-dried, low porosity and surface area gels) show almost no ability to undergo cation exchange (K_d = 6.7 for 20 ppm Pb^{2+} solution). A recent report[45] indicates that, even though xerogels still maintain some porosity after drying, most of the pores are occluded, and thus inaccessible to reactants, behaving more like a dense solid. The observation of the suppressed Pb^{2+} removal capability underscores the importance of accessible pores to the effectiveness of the cation exchange reaction.

Effect of "Real-Life" Samples on Removal Efficacy. We also tested our ZnS aerogel materials in "real-life" conditions, by treating tap water spiked with Pb^{2+} ions, to mimic a hypothetic contamination occurrence. After a 24 h contact period, the material showed similar behavior as in HPLC grade water (Table 6) removing more than 90% of the contaminant from

Table 6. Percent Removal and K_d Values for Tap Water Spiked with Different Pb^{2+} Concentrations

initial Pb^{2+} concentration (ppm)	final Pb^{2+} concentration (ppm)	removal after 24 h (%)	K_d value (mL/g)
196	2.99	98.5	6.47 × 10^4
14.7	1.17	92.0	1.15 × 10^4
0.253	0.013	94.8	1.80 × 10^4

solutions with initial concentrations ranging from 200 ppb to 200 ppm.

Quantitative Study of Hg^{2+} Removal Ability. A less detailed study was conducted on the ability of ZnS aerogels to remove Hg^{2+} from aqueous solutions. Briefly, the batch method was employed using aqueous solutions with initial concentrations ranging from 200 to 0.2 ppm. Based on the observation that the Hg^{2+} exchange occurs faster than Pb^{2+}, made during the qualitative study, samples were collected after 30 min, 1 and 3 h (Figure 7).
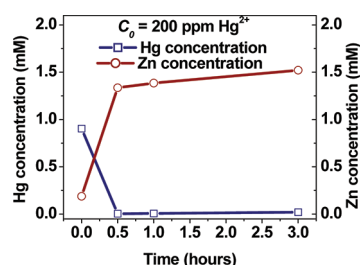
Figure 7. Decrease in Hg^{2+} and increase in Zn^{2+} concentrations as a function of contact time.

The equilibrium concentration is reached after 30 min, confirming the observed reaction speed trend. Even higher partition abilities than for the case of Pb^{2+} were observed (K_d values from 5.59 × 10^4 to 2.05 × 10^5 mL/g), as expected from the softer Lewis acid character of Hg^{2+}. A previous report[16] on a zinc tin sulfide chalcogel material has reported K_d values between 1.62 × 10^6 and 1.12 × 10^8 mL/g for the removal of Hg^{2+}, albeit using a higher volume to mass ratio (10,000 mL solution/g exchanger) and a lower initial Hg^{2+} concentration (100 ppm), which can affect the equilibrium behavior and thus preclude a direct comparison. Indeed, another report that tested layered potassium manganese sulfides using the same V/m ratio

as that used here measured K_d values closer to those that we report here (3.5 × 10^4 −3.9 × 10^5 mL/g).[14] Finally, we note that, in contrast to Pb^{2+} removal with ZnS aerogels, the presence of competing Ca^{2+} ions does not seem to affect the Hg^{2+} removal ability of the ZnS aerogel, probably also a result of the faster kinetics for Hg^{2+} uptake relative to Pb^{2+} (Table 7).

Table 7. Hg^{2+} Removal Ability for Initial Concentrations of 200 ppm and 200 ppb, and in the Presence of Excess Ca^{2+} (the maximum contaminant level in drinking water allowed by the EPA is 2 ppb Hg)

initial Hg^{2+} concentration (ppb)	final Hg^{2+} concentration (ppb)	contact time (h)	K_d value (mL/g)
1.82 × 10^5	(5.01 ± 0.80) × 10^3	3	1.95 × 10^5
329	5.99 ± 0.20	3	5.59 × 10^4
2.57 × 10^5 with 1 M Ca^{2+}	1.25 × 10^3	24	2.05 × 10^5

CONCLUSIONS

The current study has shown that ZnS aerogel materials are capable of undergoing cation exchange reactions with divalent cations (i.e., Pb^{2+}, Cd^{2+} and Hg^{2+}), directly, under very mild reaction conditions. The presence of accessible pore structure and exposed NP surfaces is paramount for the promotion of the reaction. The ZnS gel materials studied possess a characteristic dual interconnected network of nanoparticles and pores, which allows for the direct exchange between divalent cations with similar solubility to occur. This is contrary to what we and others have observed in ligand-capped metal chalcogenide nanoparticles or in xerogels where the pore structure is partially collapsed. The speed of the reaction correlates with the difference in reduction potential of the incoming versus the outgoing cation (Pb^{2+} and Hg^{2+} exchange very fast, whereas Cd^{2+} is slow and only partial exchange occurs under the same mild reaction conditions).

The quantitative study revealed that the ZnS aerogel shows the highest capacity reported to date (14.2 mmol/g) for the removal of Pb^{2+} from aqueous solutions. Distribution coefficient measurements indicate that the material is most efficient with initial Pb^{2+} concentrations in the 20−200 ppm range. This is expected, because this is an equilibrium reaction and the balance between thermodynamic and kinetic factors changes as the initial concentrations approach the solubility of the cationic species. Nevertheless, with initial concentrations around 0.1 ppm, the ZnS aerogels reduce the Pb^{2+} concentration below the 15 ppb Pb action level recommended by the EPA. In the presence of competing ions, a 1 order of magnitude decrease in the distribution coefficients is observed, but the percent removal is still more than adequate. Finally, the material shows similar efficiency in tap water spiked with Pb^{2+} contaminant, suggesting performance can be maintained in "real-life" water remediation applications.

Although the K_d values measured for the Pb^{2+} remediation are similar to those previously reported using the zinc tin sulfide chalcogel,[16] the observed overall capacity exhibited by the binary ZnS aerogel for Pb^{2+} exceeds all the other previous reports. We note that initial studies on Hg^{2+} remediation demonstrated even higher K_d values than for Pb^{2+}, as expected because of the softer Lewis acidic characteristic of Hg^{2+}, demonstrating the versatility of ZnS for Pb^{2+} and Hg^{2+} ion exchange.

The high Pb^{2+} removal capacity demonstrated by the intrinsically soft Lewis basic ZnS aerogels makes them promising for applications in fixed-bed metal-ion removal. A study of the reversibility of the ion exchange and the reusability of the material is underway, as well as a study of the long-term stability of the resulting materials. Finally, we note that the distribution coefficient values might be improved upon lowering the pH of the contaminant-containing solution, as was previously observed by other groups.[14]

■ ASSOCIATED CONTENT

Ⓢ Supporting Information

Powder X-ray diffraction spectra of the Pb^{2+}-exchanged nanoparticles (PDF). This material is available free of charge via the Internet at http://pubs.acs.org.

■ AUTHOR INFORMATION

Corresponding Author

*E-mail: sbrock@chem.wayne.edu.

Notes

The authors declare no competing financial interest.

■ ACKNOWLEDGMENTS

■ REFERENCES

(1) Nriagu, J. O.; Pacyna, J. M. *Nature* **1988**, *333* (6169), 134−139.

(2) Schwarzenbach, R. P.; Escher, B. I.; Fenner, K.; Hofstetter, T. B.; Johnson, C. A.; von Gunten, U.; Wehrli, B. *Science* **2006**, *313* (5790), 1072−1077.

(3) Dabrowski, A.; Hubicki, Z.; Podkoscielny, P.; Robens, E. *Chemosphere* **2004**, *56* (2), 91−106.

(4) Benhammou, A.; Yaacoubi, A.; Nibou, L.; Tanouti, B. *J. Colloid Interface Sci.* **2005**, *282* (2), 320−326.

(5) Nagy, N. M.; Konya, J.; Beszeda, M.; Beszeda, I.; Kalman, E.; Keresztes, Z.; Papp, K.; Cserny, I. *J. Colloid Interface Sci.* **2003**, *263* (1), 13−22.

(6) Blanchard, G.; Maunaye, M.; Martin, G. *Water Res.* **1984**, *18* (12), 1501−1507.

(7) Lagadic, I. L.; Mitchell, M. K.; Payne, B. D. *Environ. Sci. Technol.* **2001**, *35* (5), 984−990.

(8) Liu, J.; Feng, X.; Fryxell, G. E.; Wang, L.-Q.; Kim, A. Y.; Gong, M. *Adv. Mater.* **1998**, *10* (2), 161−165.

(9) Schroden, R. C.; Al-Daous, M.; Sokolov, S.; Melde, B. J.; Lytle, J. C.; Stein, A.; Carbajo, M. C.; Fernandez, J. T.; Rodriguez, E. E. *J. Mater. Chem.* **2002**, *12* (11), 3261−3267.

(10) Mercier, L.; Pinnavaia, T. J. *Environ. Sci. Technol.* **1998**, *32* (18), 2749−2754.

(11) Gash, A. E.; Spain, A. L.; Dysleski, L. M.; Flaschenriem, C. J.; Kalaveshi, A.; Dorhout, P. K.; Strauss, S. H. *Environ. Sci. Technol.* **1998**, *32* (7), 1007−1012.

(12) Bag, S.; Trikalitis, P. N.; Chupas, P. J.; Armatas, G. S.; Kanatzidis, M. G. *Science* **2007**, *317*, 490−493.

(13) Manos, M. J.; Kanatzidis, M. G. *J. Am. Chem. Soc.* **2009**, *131* (18), 6599−6607.

(14) Manos, M. J.; Kanatzidis, M. G. *Chem.—Eur. J.* **2009**, *15* (19), 4779−4784.

(15) Ding, N.; Kanatzidis, M. G. *Nat. Chem.* **2010**, *2* (3), 187−191.

(16) Oh, Y.; Bag, S.; Malliakas, C. D.; Kanatzidis, M. G. *Chem. Mater.* **2011**, *23* (9), 2447−2456.

(17) Borah, D.; Senapati, K. *Fuel* **2006**, *85* (12−13), 1929−1934.

(18) Erdem, M.; Ozverdi, A. *Sep. Purif. Technol.* **2006**, *51* (3), 240−246.

(19) Ozverdi, A.; Erdem, M. *J. Hazard. Mater.* **2006**, *137* (1), 626−632.

(20) Wark, S. E.; Hsia, C.; Son, D. H. *J. Am. Chem. Soc.* **2008**, *130*, 9550−9555.

(21) Son, D. H.; Hughes, S. M.; Yin, Y.; Paul Alivisatos, A. *Science* **2004**, *306* (5698), 1009−1012.

(22) Yao, Q.; Arachchige, I. U.; Brock, S. L. *J. Am. Chem. Soc.* **2009**, *131*, 2800−2801.

(23) Gacoin, T.; Malier, L.; Boilot, J.-P. *Chem. Mater.* **1997**, *9*, 1502−1504.

(24) Gacoin, T.; Malier, L.; Boilot, J.-P. *J. Mater. Chem.* **1997**, *7*, 859−860.

(25) Gacoin, T.; Lahlil, K.; Larregaray, P.; Boilot, J.-P. *J. Phys. Chem. B* **2001**, *105*, 10228−10235.

(26) Arachchige, I. U.; Brock, S. L. *Acc. Chem. Res.* **2007**, *40* (9), 801−809.

(27) Gaponik, N.; Wolf, A.; Marx, R.; Lesnyak, V.; Schilling, K.; Eychmüller, A. *Adv. Mater.* **2008**, *20*, 4257−4262.

(28) Yao, Q.; Brock, S. L. *Nanotechnol.* **2010**, *21* (11), 115502.

(29) Pala, I. R.; Arachchige, I. U.; Georgiev, D. G.; Brock, S. L. *Angew. Chem., Int. Ed.* **2010**, *49* (21), 3661−3665.

(30) Mertz, W., *Trace Elements in Human and Animal Nutrition*, 5th ed.; Academic Press: Orlando, 1986.

(31) Licht, S. *J. Electrochem. Soc.* **1988**, *135* (12), 2971−2975.

(32) West, A. R., *Basic Solid State Chemistry*, 2nd ed.; John Wiley & Sons: New York, 1999.

(33) Fedorov, V. A.; Ganshin, V. A.; Korkishko, Y. N. *Phys. Status Solidi* **1993**, *139* (9), 9−65.

(34) Li, H.; Zanella, M.; Genovese, A.; Povia, M.; Falqui, A.; Giannini, C.; Manna, L. *Nano Lett.* **2011**, *11* (11), 4964−4970.

(35) Engelken, R. D.; Ali, S.; Chang, L. N.; Brinkley, C.; Turner, K.; Hester, C. *Mater. Lett.* **1990**, *10* (6), 264−274.

(36) Mews, A.; Eychmueller, A.; Giersig, M.; Schooss, D.; Weller, H. *J. Phys. Chem.* **1994**, *98* (3), 934−941.

(37) Jain, P. K.; Amirav, L.; Aloni, S.; Alivisatos, A. P. *J. Am. Chem. Soc.* **2010**, *132* (29), 9997−9999.

(38) Luther, J. M.; Zheng, H.; Sadtler, B.; Alivisatos, A. P. *J. Am. Chem. Soc.* **2009**, *131* (46), 16851−16857.

(39) Rivest, J. B.; Swisher, S. L.; Fong, L.-K.; Zheng, H.; Alivisatos, A. P. *ACS Nano* **2011**, *5* (5), 3811−3816.

(40) Arachchige, I. U.; Brock, S. L. *J. Am. Chem. Soc.* **2006**, *128* (24), 7964−7971.

(41) Helfferich, F. *Ion Exchange*; McGraw-Hill Book Company: New York, 1962; p 2.

(42) Chan, E. M.; Marcus, M. A.; Fakra, S.; ElNaggar, M.; Mathies, R. A.; Alivisatos, A. P. *J. Phys. Chem. A* **2007**, *111* (49), 12210−12215.

(43) Tang, Z.; Podsiadlo, P.; Sup Shim, B.; Lee, J.; Kotov, N. A. *Adv. Funct. Mater.* **2008**, *18*, 3801−3808.

(44) Fryxell, G. E.; Lin, Y.; Fiskum, S.; Birnbaum, J. C.; Wu, H.; Kemner, K.; Kelly, S. *Environ. Sci. Technol.* **2005**, *39* (5), 1324−1331.

(45) Pawsey, S.; Kalebaila, K. K.; Moudrakovski, I.; Ripmeester, J. A.; Brock, S. L. *J. Phys. Chem. C* **2010**, *114* (31), 13187−13195.